Vibration Attenuation in Layered and Welded Beams with Unequal Thickness

B. Singh, K. K. Agrawal and B. K. Nanda

***Abstract*—**In built-up structures, one of the effective ways of dissipating unwanted vibration is to exploit the occurrence of slip at the interfaces of structural laminates. The present work focuses on the dynamic analysis of welded structures. A mathematical formulation has been developed for the mechanism of slip damping in layered and welded mild steel beams with unequal thickness subjected to both periodic and non-periodic forces. It is observed that a number of vital parameters such as; thickness ratio, pressure distribution characteristics, relative slip and kinematic co-efficient of friction at the interfaces, nature of exciting forces, length and thickness of the beam specimen govern the damping characteristics of these structures. Experimental verification has been carried out to validate the analysis and study the effect of these parameters. The developed damping model for the structure is found to be in fairly good agreement with the measured data. Finally, the results of the analysis are discussed and rationalized.

***Keywords*—**Slip damping, tack welded joint, thickness ratio, in-plane bending stress

I. Introduction

WELDED joints are often used to assemble the fabricated structures. These joints have a great potential to reduce the vibration levels of these structures, thereby attracting the interest of many researchers to understand the mechanism of vibration attenuation. Goodman and Klumpp [1] examined the energy dissipation due to slip at the interfaces of a laminated beam. Studies by researchers such as; Goodman [2], Earles [3], Murty [4] have shown that the energy dissipation at the joints occur due to interfacial friction which is more than the energy loss at the support. In fact following the work of Goodman and Klumpp [1], early researchers, such as Masuko et al [5] and Nishiwaki et al. [6], studied the damping capacity of layered and bolted structures assuming uniform intensity of pressure distribution at the interfaces. However, their work is limited to the layered and jointed symmetric structures vibrating under static conditions. Nanda [7] examined the interfacial slip damping in multilayered bolted structures and developed a theoretical expression for the pressure distribution at the interfaces of a bolted joint by curve fitting the earlier data reported by Ziada and Abd [8]. They further studied the vibration characteristics of bolted structures and established the effects of number of layers, diameter of bolts and use of washers on the damping capacity.

B. Singh is with the Mechanical Engineering Department, Sir Padampat Singhania University, Udaipur, Rajasthan-313601, India. (e-mail: bhagat.singh@spsu.ac.in).

K. K. Agrawal is with the Mechanical Engineering Department, Sir Padampat Singhania University, Udaipur, Rajasthan-313601, India. (e-mail: kamal.agrawal@spsu.ac.in).

B. K. Nanda with the Mechanical Engineering Department, National Institute of Technology, Rourkela, Odisha, India.

In their analysis they neglected the effect of in-plane bending stresses on the slip considering the damping capacity of layered and bolted structures with symmetric cantilever beams vibrating under static conditions.

The effect of non-uniform interface pressure distribution on the mechanism of slip damping for layered and jointed beams vibrating at static conditions has been examined recently by Damisa et al. [9]. Damisa et al. [10] also examined the effect of non-uniform interface pressure distribution on the mechanism of slip damping for layered beams under dynamic loads. Though these researchers considered the in-plane distribution of bending stresses but all these analyses are limited to the symmetric structures with single interface.

Although a lot of work has been carried out on the damping capacity of bolted structures, little work has been reported on the mechanism of damping in layered and welded structures. Recently, Singh and Nanda [11] proposed a method to evaluate the damping capacity of tack welded structures. They established that with the increase in the number of tack welds the damping capacity decreases.

II. Static Analysis

The two layered and tack welded cantilever beam model with overall thickness 2*h*, width *b* and length *l* as shown in Fig. 1(a) is considered to find out the damping ratio. The loading consists of uniformly distributed pressure at the interfaces due to contact between two flat bodies, and a concentrated load P is applied at the free end, x= *l*. Each of the two halves of thickness h_1 and h_2 is considered separately with the loading as depicted in the Fig. 1(b). The continuity of stress and vertical displacement '*v*' is imposed at the interfaces. At some finite value of *P*, the shear stress at the interfaces will reach the critical value for slip $\tau_{xy} = \mu p$, where μ and p are the kinematic co-efficient friction and interface pressure respectively. Additional static force due to excitation will produce a relative displacement $\Delta u(x)$ at the interfaces.

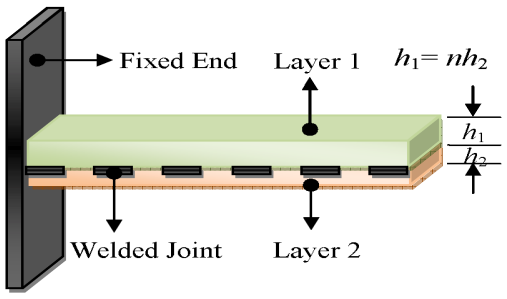

Fig. 1 (a) Two layered tack welded cantilever beam model

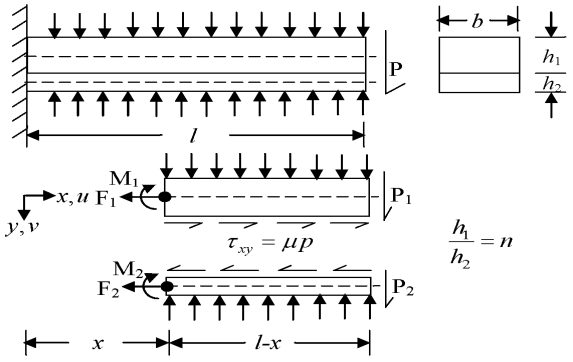

Fig. 1(b) Two halves of the beam depicting load

A. Interface Pressure Distribution

Contrary to this, the pressure distribution at the interfaces is assumed to be uniform owing to the contact of the upper layer over the lower one. Therefore, the relation for uniform pressure distribution as given by Johnson [12] and Giannakopoulos et al. [13] due to contact of two flat bodies has been considered and the same is given by;

$$p(x)=\frac{P}{b} \tag{1}$$

where *P* and *b* are the normal load per unit length and width of the beam respectively.

B. Analysis of Static Response

The static response is evaluated considering the jointed structure fabricated with cantilever beams of unequal thickness. The ratio of the two layers considered is given by;

$$\frac{h_1}{h_2}=n \tag{2}$$

where h_1, h_2 are the thickness of the upper and lower layers respectively and *n* is a constant.

Furthermore,

$$h_1+h_2=2h \tag{3}$$

Solving expressions (2) and (3), thickness of the upper and lower layers is given by;

$$h_1=2hn/n+1 \tag{4a}$$

$$h_2=2h/n+1 \tag{4b}$$

The resultant moment at the centroid of each laminate as shown in Fig.1 (b) is given by;

$$M_1=P_1(l-x)-\mu pb\frac{nh}{n+1}(l-x) \tag{5a}$$

$$M_2=P_2(l-x)-\mu pb\frac{h}{n+1}(l-x) \tag{5b}$$

where the subscripts 1 and 2 refer to the upper and lower laminates respectively. Moreover, P_1 and P_2 are the static forces acting on the laminates 1 and 2 respectively as shown in Fig. 1(b).

Furthermore,

$$P_1+P_2=P \tag{6}$$

Invoking the relation between bending moment and curvature we get;

$$M=-EI\frac{\mathrm{d}^2v}{\mathrm{d}x^2} \tag{7}$$

where *E* is the modulus of elasticity

Putting expression (5) in (7), the following expression is obtained;

$$\frac{\mathrm{d}^2v_1}{\mathrm{d}x^2}=\frac{1}{EI_1}\left(P_1-\frac{\mu pbnh}{n+1}\right)(l-x) \tag{8a}$$

$$\frac{\mathrm{d}^2v_2}{\mathrm{d}x^2}=\frac{1}{EI_2}\left(P_2-\frac{\mu pbh}{n+1}\right)(l-x) \tag{8b}$$

where, $I_1\left(bh_1^3/12\right)$, $I_2\left(bh_2^3/12\right)$, v_1 and v_2 are the moment of inertia and static response of the laminates 1 and 2 respectively.

Integrating expression (8) once we get;

$$\frac{\mathrm{d}v_1}{\mathrm{d}x}=\frac{1}{EI_1}\left(P_1-\frac{\mu pbnh}{n+1}\right)\left(lx-\frac{x^2}{2}\right)+C_{1a} \tag{9a}$$

$$\frac{\mathrm{d}v_2}{\mathrm{d}x}=\frac{1}{EI_2}\left(P_2-\frac{\mu pbh}{n+1}\right)\left(lx-\frac{x^2}{2}\right)+C_{1b} \tag{9b}$$

where C_{1a}, C_{1b} are the integration constant and is evaluated to be zero by putting the boundary condition, $\left(\mathrm{d}v_1/\mathrm{d}x\right)\Big|_{x=0}=\left(\mathrm{d}v_2/\mathrm{d}x\right)\Big|_{x=0}=0$ in the expression (9).

Further, integration of expression (9) yields;

$$v_1=\frac{3(n+1)^3}{2Ebh^3n^3}\left(P_1-\frac{\mu pbhn}{n+1}\right)\left(\frac{lx^2}{2}-\frac{x^3}{6}\right)+C_{2a} \tag{10a}$$

$$v_2=\frac{3(n+1)^3}{2Ebh^3}\left(P_2-\frac{\mu pbh}{n+1}\right)\left(\frac{lx^2}{2}-\frac{x^3}{6}\right)+C_{2b} \tag{10b}$$

where the integration constants, $C_{2a}=C_{2b}=0$

since $v_1\big|_{x=0}=v_2\big|_{x=0}=0$.

Furthermore, it is assumed that the continuity equation prevails as such;

$$v_1=v_2 \tag{11}$$

Solving expressions (10) and (11) we get;

$$P_1=\frac{n^3P+n\left(2n^3-n+1\right)Q}{n^3+1} \tag{12a}$$

$$P_2=\frac{P+n(n-1)Q}{n^3+1} \tag{12b}$$

The two dimensional parameters Q and R are defined as;

$$Q=\mu pbh \tag{13a}$$

$$R=\frac{Ebh^3}{l^3} \tag{13b}$$

Using the expressions (10), (12) and (13), the static response in terms of "Q" and "R" are finally found to be;

$$v_1=v_2=\frac{(n+1)^3}{4R\left(n^3+1\right)}(P-Q)\left[3\left(\frac{x}{l}\right)^2-\left(\frac{x}{l}\right)^3\right] \tag{14}$$

C. Evaluation of Relative Slip

The displacement at any axial position x and $y_{1,2} = \mp h/2$ are given by;

$$u_1 = \frac{1}{E}\int_0^x \sigma_{x_1}\,\mathrm{d}x - \frac{h_1}{2}\frac{\mathrm{d}v_1}{\mathrm{d}x} \tag{15a}$$

$$u_2 = \frac{1}{E}\int_0^x \sigma_{x_2}\,\mathrm{d}x + \frac{h_2}{2}\frac{\mathrm{d}v_2}{\mathrm{d}x} \tag{15b}$$

These displacements are produced by the resultant axial force $F_{1,2}$ and moment $M_{1,2}$ about the centroid of each half of the beam as shown in Fig.1 (b). The parameters v_1, v_2 are the vertical deflections, E is the modulus of elasticity and $\sigma_{x_1}, \sigma_{x_2}$ are the in-plane bending stresses. It is assumed that the continuity equation prevails, i.e., $v_1 = v_2 = v$

From the force equilibrium, the in-plane bending stresses in the upper and lower laminates are computed as:

$$\sigma_{x_1} = \frac{\mu p(n+1)}{2nh}(l-x) \tag{16a}$$

$$\sigma_{x_2} = -\frac{\mu p(n+1)}{2h}(l-x) \tag{16b}$$

Combining expressions (14), (15) and (16) and simplifying, the relative slip displacement at the interfaces is given by;

$$\Delta u = u_2 - u_1 = \frac{3(n+1)^3 h}{4\left(n^3+1\right)Rl}\left[P - \frac{\left(n^3+3n^2+3n+1\right)}{3n(n+1)}Q\right]\times \left[2\left(\frac{x}{l}\right)-\left(\frac{x}{l}\right)^2\right] \tag{17}$$

Slip will occur only if $P > P_c = \dfrac{\left(n^3+3n^2+3n+1\right)}{3n(n+1)}Q$.

where, P_c is the critical static load. This is the minimum load required to initiate slip.

III. Dynamic Analysis

For the forced vibration of a cantilever beam, the static analysis has been extended to include distributed inertia forces and examine their effect on the mode shape, slip distribution and energy dissipation due to slip. The present formulation is the extension of static analysis as depicted in the preceding section for the beam as shown in Fig. 1.

A. Analysis of Dynamic response

The forced vibration of the beam produced by a time-dependent displacement at the unsupported end has been considered such that;

$$v\big|_{x=l} = f(t) \tag{18}$$

Following Timoshenko [14], the dynamic displacement is composed of two parts;

$$v = v_{\mathrm{I}} + v_{\mathrm{II}} \tag{19}$$

where

$$v_{\mathrm{I}} = \frac{9}{8}\frac{(n+1)^3}{\left(n^3+1\right)}\left[\frac{3}{2}\left(\frac{x}{l}\right)^2 - \frac{1}{2}\left(\frac{x}{l}\right)^3\right] f(t) \tag{20}$$

The term in the bracket represents the static mode function and satisfies the end conditions;

$$v_{\mathrm{I}}\big|_{x=0} = 0; \left.\frac{\mathrm{d}v_{\mathrm{I}}}{\mathrm{d}x}\right|_{x=0} = 0; \left.\frac{\mathrm{d}^2 v_{\mathrm{I}}}{\mathrm{d}x^2}\right|_{x=l} = 0; v_{\mathrm{I}}\big|_{x=l} = 0; \tag{21}$$

but not the dynamic equilibrium equation;

$$EI\frac{\partial^4 v}{\partial x^4} + \rho A\frac{\partial^2 v}{\partial t^2} = 0 \tag{22}$$

where, EI and ρ are the flexural rigidity and density of the beam, respectively.

The displacement v_{I} produces the dynamic loads as given by;

$$-\frac{9}{8}\frac{(n+1)^3}{\left(n^3+1\right)}A\rho\left[\frac{3}{2}\left(\frac{x}{l}\right)^2 - \frac{1}{2}\left(\frac{x}{l}\right)^3\right]\ddot{f}(t) \tag{23}$$

where A is the cross-sectional area of the beam.

Moreover, the displacement (v_{II}) representing vibrations produced by the force function (23) is expressed as;

$$v_{\mathrm{II}} = \sum_i \varphi_i(t)\,X_i(x) \tag{24}$$

where $X_i(x)$ and $\varphi_i(t)$ are the modal and time-dependent functions, respectively.

v_{II} must satisfy the end conditions;

$$v_{\mathrm{II}}\big|_{x=0} = 0; \left.\frac{\mathrm{d}v_{\mathrm{II}}}{\mathrm{d}x}\right|_{x=0} = 0; \left.\frac{\mathrm{d}^2 v_{II}}{\mathrm{d}x^2}\right|_{x=l} = 0; v_{\mathrm{II}}\big|_{x=l} = 0; \tag{25}$$

$X_i(x)$ are the solutions of the expression (22) and satisfies the end condition as given in (25). Thus we get;

$$X_i = \sinh k_i l \sin k_i(l-x) - \sin k_i l \sinh k_i(l-x) \tag{26}$$

where k_i are the roots of the following expression;

$$\tanh k_i l = \tan k_i l \tag{27}$$

The total displacement is then given by;

$$v = \frac{9}{8}\frac{(n+1)^3}{\left(n^3+1\right)}\left[\frac{3}{2}\left(\frac{x}{l}\right)^2 - \frac{1}{2}\left(\frac{x}{l}\right)^3\right] f(t) + \sum_i \varphi_i(t) X_i(x) \tag{28}$$

Applying the principle of virtual work, Timoshenko [14] has shown that the time-dependent functions $\varphi_i(t)$ must satisfy the differential equation

$$\ddot{\varphi}_i + \frac{EIk_i^4}{A\rho}\varphi_i = -b_i\ddot{f}(t) \tag{29}$$

where the dot superscripts denote differentiation with respect to time. The coefficients b_i are obtained by expanding the force function (23) in a series of the normal functions, X_i. Thus,

$$-\frac{9}{8}\frac{(n+1)^3}{\left(n^3+1\right)}A\rho\ddot{f}(t)\left[\frac{3}{2}\left(\frac{x}{l}\right)^2 - \frac{1}{2}\left(\frac{x}{l}\right)^3\right] = -A\rho\ddot{f}(t)\sum_i b_i X_i \tag{30}$$

and the coefficients b_i are obtained from the following expression;

$$b_i = \frac{\int_0^l \frac{9}{8}\frac{(n+1)^3}{(n^3+1)}\{X_i\}\left[\frac{3}{2}\left(\frac{x}{l}\right)^2 - \frac{1}{2}\left(\frac{x}{l}\right)^3\right] \mathrm{d}x}{\int_0^l X_i^2 \,\mathrm{d}x} \tag{31}$$

Integrating the expression (31) b_i is finally found to be;

$$b_i = \frac{9(n+1)^3}{4(n^3+1)k_i l(\sinh k_i l - \sin k_i l)} \tag{32}$$

The general solution of expression (29) is given by;

$$\varphi_i(t) = A_i \cos p_i t + B_i \sin p_i t - \frac{b_i}{p_i}\int_0^t \ddot{f}(t)\sin p_i(t-\tau)\mathrm{d}\tau \tag{33}$$

where

$$p_i = \left(\frac{EI}{A\rho}\right)^{1/2} k_i^2$$

Constants A_i and B_i are evaluated from the initial conditions;

$$v(0) = U(x,0) \tag{34a}$$

$$\dot{v}(0) = V(x,0) \tag{34b}$$

Putting expression (28) in (34), U and V are evaluated as;

$$U = \frac{9}{8}\frac{(n+1)^3}{(n^3+1)}\left[\frac{3}{2}\left(\frac{x}{l}\right)^2 - \frac{1}{2}\left(\frac{x}{l}\right)^3\right] f(0) + \sum_i X_i\{A_i\} \tag{35a}$$

$$V = \frac{9}{8}\frac{(n+1)^3}{(n^3+1)}\left[\frac{3}{2}\left(\frac{x}{l}\right)^2 - \frac{1}{2}\left(\frac{x}{l}\right)^3\right] \dot{f}(0) + \sum_i X_i\{B_i p_i\} \tag{35b}$$

Moreover;

$$\frac{9}{8}\frac{(n+1)^3}{(n^3+1)}\left[\frac{3}{2}\left(\frac{x}{l}\right)^2 - \frac{1}{2}\left(\frac{x}{l}\right)^3\right] = \sum_i b_i X_i \tag{36}$$

Putting expression (36) in (35) and simplifying we get;

$$U(x,0) = \sum_i X_i\{A_i + b_i f(0)\} \tag{37a}$$

$$V(x,0) = \sum_i X_i\{B_i p_i + b_i \dot{f}(0)\} \tag{37b}$$

Putting the initial conditions U=V=0, the constants A_i and B_i are found as;

$$A_i = -b_i f(0) \tag{38a}$$

$$B_i = -\frac{b_i}{p_i}\dot{f}(0) \tag{38b}$$

Substitution of expressions (33) and (38) in (28) yields;

$$v(x,t) = \frac{9}{8}\frac{(n+1)^3}{(n^3+1)}\left[\frac{3}{2}\left(\frac{x}{l}\right)^2 - \frac{1}{2}\left(\frac{x}{l}\right)^3\right] f(t) - f(0)\sum_i b_i X_i \cos p_i t - \dot{f}(0)\sum_i \frac{b_i}{p_i} X_i \sin p_i t - \sum_i \frac{b_i}{p_i} X_i \int_0^t \ddot{f}(\tau)\sin p_i(t-\tau)\mathrm{d}\tau \tag{39}$$

Integrating and simplifying the expression (39), the transverse deflection is finally found to be;

$$v(x,t) = \frac{9}{8}\frac{(n+1)^3}{(n^3+1)}\left[\frac{3}{2}\left(\frac{x}{l}\right)^2 - \frac{1}{2}\left(\frac{x}{l}\right)^3\right] f(t) - \sum_i b_i X_i f(t) + \sum_i b_i X_i p_i \int_0^t f(\tau)\sin p_i(t-\tau)\mathrm{d}\tau \tag{40}$$

B. Evaluation of Dynamic Slip

The relative slip at the interfaces under dynamic condition is evaluated by combining the expressions (15), (16) and (40). The relative slip at the interfaces is given by;

$$\Delta u_x = u_2 - u_1 = -\frac{9(n+1)^3 \mu p l^2}{8(n^3+1)Eh}\left(\frac{2x}{l} - \frac{x^2}{l^2}\right) + h\frac{\mathrm{d}v}{\mathrm{d}x} \tag{41}$$

Utilizing the expression for mode shape as given by (40) in (41), the relative slip is modified as;

$$\Delta u_x = \frac{9}{8}\frac{(n+1)^3}{(n^3+1)}\left[-\frac{\mu p l^2}{Eh} + \frac{3h}{2l} f(t)\right]\left(\frac{2x}{l} - \frac{x^2}{l^2}\right) + h\sum_i b_i k_i\left[\sinh k_i l\cos k_i(l-x) - \sin k_i l\cosh k_i(l-x)\right] \times\left[f(t) - p_i\int_0^t f(\tau)\sin p_i(t-\tau)\mathrm{d}\tau\right] \tag{42}$$

C. Analysis of Energy Dissipated

The energy is dissipated due to friction and relative dynamic slip at the interfaces. For completely reversed loading, the product of the shear force, μp and the relative displacement, Δu is integrated over the length of the beam which is found to be equal to one-fourth of the energy dissipation in a complete cycle.

Thus, energy dissipation per cycle as established by Goodman and Klumpp (1956) is given by;

$$E_{loss} = 4b\int_0^l \tau_{xy}\Delta u(x)\mathrm{d}x = 4\mu pb\int_0^l (u_2 - u_1)\mathrm{d}x \tag{43}$$

where, u_1 and u_2 are the displacements in the x-direction of points on the adjacent faces of the upper and lower half beam respectively.

Substituting the expression (42) in (43) and integrating, the energy dissipation per cycle is given by;

$$E_{loss} = 4\mu pbh\left[f(t) - \frac{(n+1)^2}{6n}\frac{\mu p l^2}{Eh^2}\right] \tag{44}$$

The expression (44) is modified putting two dimensional parameters Q and R as given by expressions {13(a) and 13 (b)} and the same is given as;

$$E_{loss} = 4Q\left(f(t) - \frac{(n+1)^2}{6n}\frac{Q}{R}\right) \tag{45}$$

D. Evaluation of Loss Factor

In vibration problems, it is most convenient to express the dissipative properties of the system in terms of non-

dimensional quantities such as the damping ratio ψ and loss factor η_s, defined by;

$$\psi = \frac{E_{loss}}{E_{ne}} \tag{46a}$$

$$\eta_s = \frac{E_{loss}}{2\pi E_{ne}} = \frac{\psi}{2\pi} \tag{46b}$$

where, E_{ne} is the maximum strain energy stored in the system. The maximum strain energy stored in the system in terms of dynamic deflection at the tip of the beam is given by;

$$E_{ne} = \frac{1}{2}k\left[f(t)\right]^2 = R\left[f(t)\right]^2 \tag{47}$$

where $\left(k = \frac{3EI}{l^3}\right)$ is the bending stiffness

Putting expressions (45) and (47) in expression 46 (a) and simplifying, the damping ratio in terms of dynamic tip displacement is given by;

$$\psi = \frac{4Q}{R\left[f(t)\right]^2}\left(f(t) - \frac{(n+1)^2}{6n}\frac{Q}{R}\right) \tag{48}$$

Putting expression (48) in expression 46(b) and simplifying, the loss factor in terms of dynamic tip displacement is given as;

$$\eta_s = \frac{2Q}{\pi R\left[f(t)\right]^2}\left(f(t) - \frac{(n+1)^2}{6n}\frac{Q}{R}\right) \tag{49}$$

This result clearly indicates that the value for expression (49) cannot be fully determined until the forcing time dependent displacement function *f (t)* is fully specified. Consequently, we limit our analysis to the following case namely:
where ω is the excitation frequency

(a) $f(t) = F_0 H(t - t_0)$ (50a)

where $H(t)$ is the Heaviside function and $F0$ is the amplitude

(b) $f(t) = F_0 e^{i\omega t}$ (50b)

The dynamic response, slip and the loss factor have been evaluated for the above cases of $f(t)$ putting the expressions {50(a) and 50(b)} in (40), (42) and (49).

IV. Experimental Setup and Experiments

An experimental set-up as shown in Fig. 2 has been fabricated to conduct the experiments. The specimens are prepared from the stock of mild steel flats by tack welding two layers of various thickness and cantilever length. The details of the mild steel specimen used for experimentation are given in Table 1. The cantilever specimens are excited transversally by a time dependent displacement at the free end with the help of vibration generator. The input excitation and output vibration are sensed with vibration pick-ups and the corresponding signal is fed to a digital storage oscilloscope which is connected to the computer with vibration analyzer software i. e., Lab View of National Instruments limited.

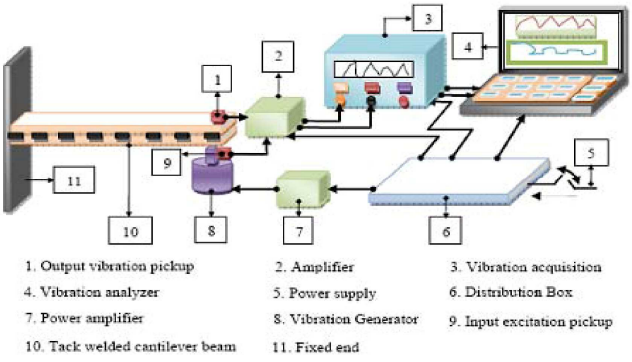

Fig. 2 Experimental setup

TABLE I
Details of Mild Steel Specimens

Thickness of the specimen (h_1+h_2) (mm)	Width of the specimen (mm)	Cantilever length (mm)	Type of welding
(6+6)	40.2	520.6	Tack Welding
(8+4)	40.2		
(9+3)	40.2		
(10+2)	40.2		
(6+6)	40.2	560.4	Tack Welding
(8+4)	40.2		
(9+3)	40.2		
(10+2)	40.2		
(6+6)	40.2	600.6	Tack Welding
(8+4)	40.2		
(9+3)	40.2		
(10+2)	40.2		

The frequency response has been generated for the first four modes of the vibration. The frequency response curves at different loadings are shown in Figs. 3 and 4. The experimental damping ratio is then evaluated using experimental FRF curves.

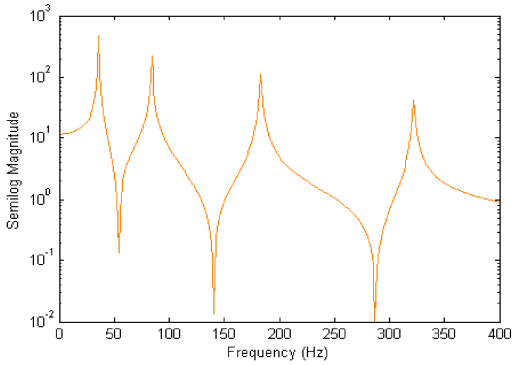

Fig. 3 FRF plot at harmonic loading for jointed and welded cantilever beams of dimensions=600.6×40.2×3 mm^3

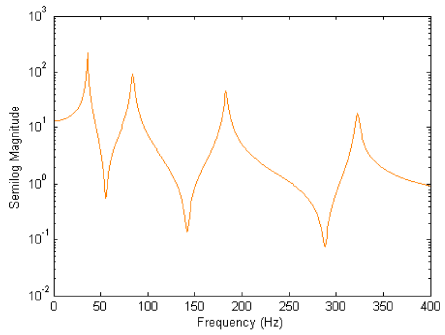

Fig. 4 FRF plot at Heaviside loading for jointed and welded cantilever beams of dimensions=600.6×40.2×3 mm^3

V. RESULTS AND DISCUSSION

The loss factor for two layered and tack welded mild steel specimens of unequal thickness have been found out numerically using the expression (49). From this analysis the following inferences have been drawn as detailed below. Energy loss in the welded structures with various thickness ratios for a particular configuration has been plotted in the Fig. 5.

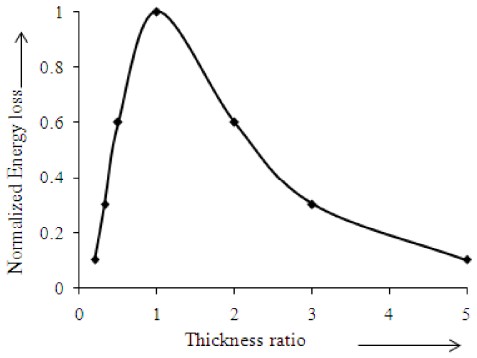

Fig. 5 Variation of Energy loss with thickness ratio for welded cantilever beams

All other parameters remaining constant, with thickness ratio greater than one, initiation of slip requires a larger displacement and the energy loss reduces compared to the jointed beam of equal thickness. In other words, energy dissipation is maximized by having the slip interface at the centroid of the total beam cross-section. The variation of critical load and amplitude has been plotted in Fig. 6.

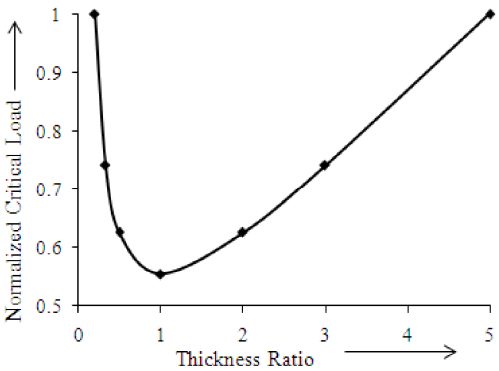

Fig. 6(a) Variation of critical load with thickness ratio for welded cantilever beams

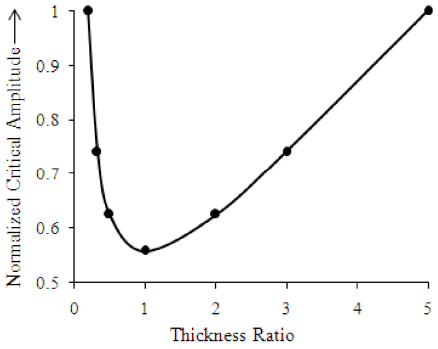

Fig. 6(b) Variation of critical amplitude with thickness ratio for welded cantilever beams

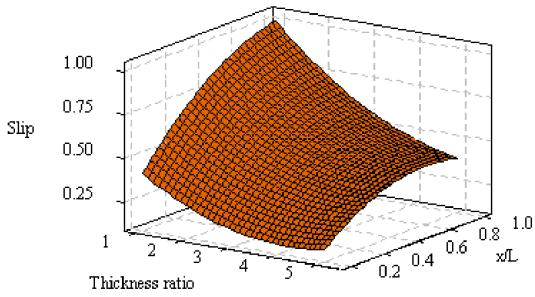

Fig. 7 Surface plot of normalized slip with axial position and thickness ratio

From the plots it is evident that the critical load and amplitude increases with the increase in thickness ratio. The variation of relative slip with an axial distance from the fixed end has been plotted in Fig. 7. From the figure it is quite evident that the relative slip increases with the distance from the fixed end. Moreover, the relative slip is maximum at thickness ratio of one and decreases as the ratio is increased. In welded beams of equal thickness the slip surface is at the centroid of the total beam cross-section.

It is evident from the expression (49) that for the beam with the same total thickness, the loss coefficient is increased by having laminates of equal thickness. However, for jointed beam with laminates of unequal thickness, the onset of slip is delayed due to higher critical load, as compared to that of the laminates of equal thickness as evident from the expressions (17) and (42). The reason being, slip interface is not at the centroid of the beam in case of layered and welded non-symmetric beams thereby raising the critical load.

The variation of energy loss with the initial amplitude of excitation for the layered and jointed beams of symmetric and non-symmetric beams has been plotted in Fig. 8. From the figure it is apparent that the energy dissipation increases with the increase in initial amplitude of excitation. From the expression (45) it is deduced that the energy loss due to friction is directly proportional to the initial amplitude of excitation which establishes that energy dissipation is enhanced with increase in initial amplitude of excitation. Further, the relative slip at the interfaces is increased due to increase in initial amplitude of excitation as shown in expressions (17) and (42), thereby enhancing the energy loss due to friction.

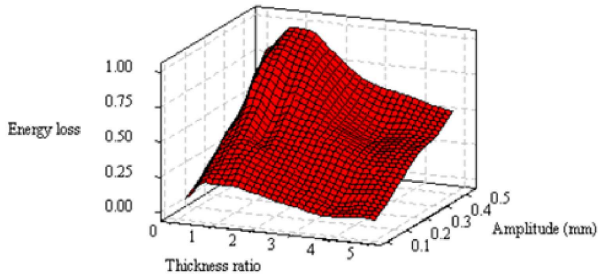

Fig. 8 Surface plot of normalized energy loss with amplitude and thickness ratio

The dynamic response of the two layered welded beams with various thickness ratios have been shown in the Figs. 9 and 10. From the figure it is evident that the dynamic response decreases with the increase in the thickness ratio.

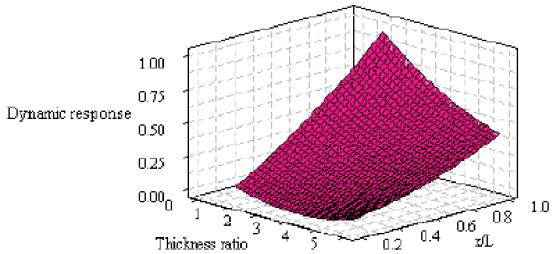

Fig. 9 Surface plot of dynamic response with axial position and thickness ratio greater than one

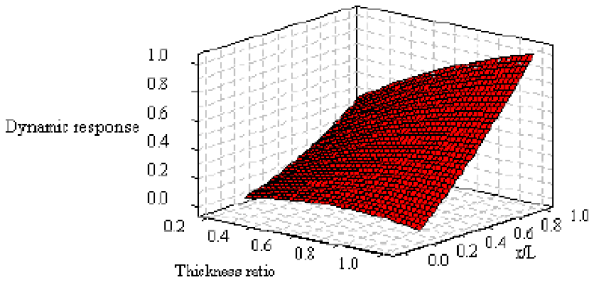

Fig. 10 Surface plot of dynamic response with axial position and thickness ratio less than one

The variation of relative slip with an axial distance from the fixed end and normalized time has been plotted in Figs. 11 and 12. From the figures it is quite evident that the relative slip increases with the distance from the fixed end and is maximum at the free end.

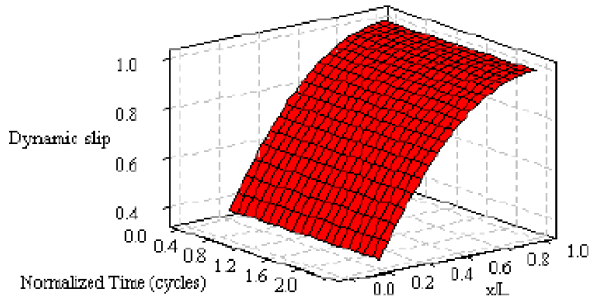

Fig. 11 Normalized slip profile at Heaviside loading for jointed and welded cantilever beams

The variation of dynamic response with an axial distance from the fixed end and normalized time has been plotted in Figs. 13 and 14. From the figures it is inferred that the dynamic response increases with the distance from the fixed end and is maximum at the unsupported end.

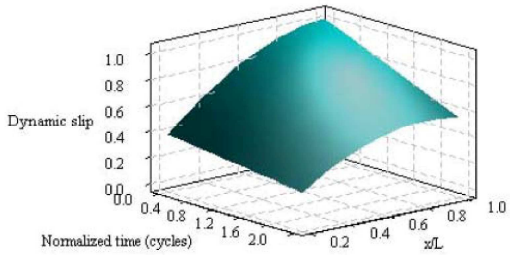

Fig. 12 Normalized slip profile at harmonic loading for jointed and welded cantilever beams

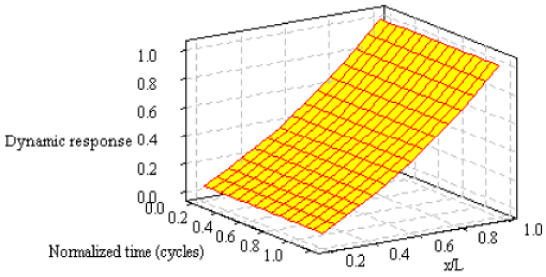

Fig. 13 Normalized dynamic response profile at Heaviside loading for welded cantilever beams

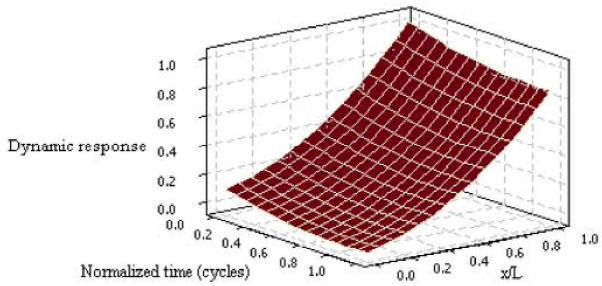

Fig. 14 Normalized dynamic response profile at harmonic loading for welded cantilever beams

The variation of relative slip with respect to axial distance from the fixed end versus frequency ratio for Heaviside and harmonic loading have been plotted in Figs. 15 and 16, respectively. From the figures it is concluded that the relative slip increases with the distance from the fixed end and is maximum at the unsupported end. Moreover the relative slip increases in the pre-resonance region with the increasing frequency and is maximum at the frequency ratio of one, i. e., at the resonant frequency. The variation of dynamic response with respect to axial distance from the fixed end versus frequency ratio for Heaviside and harmonic loading have been plotted in Figs. 17 and 18 respectively. It is evident that the dynamic response increases with the distance from the fixed end and is maximum at the unsupported end. Moreover the dynamic response is maximum at the resonant frequency, i. e., at the frequency ratio of one.

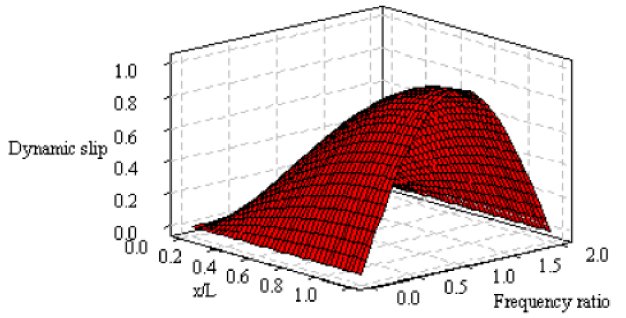

Fig. 15 Normalized slip profile at Heaviside loading with respect to the frequency ratio

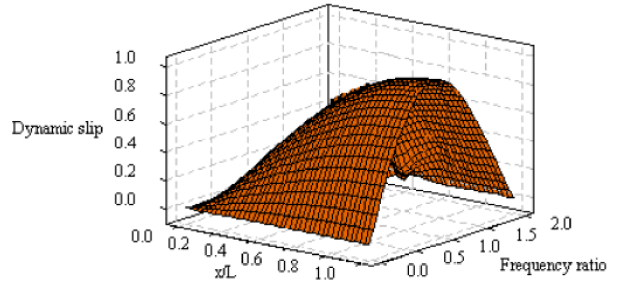

Fig. 16 Normalized slip profile at harmonic loading with respect to the frequency ratio

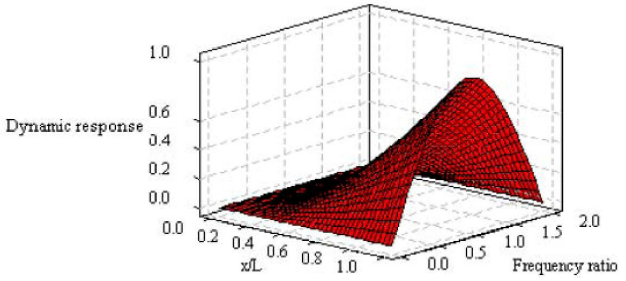

Fig. 17 Normalized dynamic response at Heaviside loading with respect to the frequency ratio

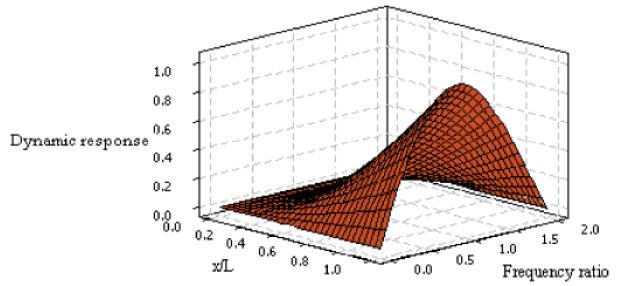

Fig. 18 Normalized dynamic response at harmonic loading with respect to the frequency ratio

The theoretical loss factor has been evaluated for various configurations and vibration conditions using the expression (49) and plotted along with the corresponding experimental ones as solid (——) and dotted lines (------) as shown in Figs. 19 to 21 respectively for comparison. It is observed that both the curves are in good agreement with a maximum variation of 9.8% which authenticates the theoretical analysis. Fig. 19 shows that the loss factor decreases with the increase in the initial amplitude of vibration at the free end of the beam model although increase in the amplitude of vibration raises energy loss due to friction. The strain energy introduced into the system is proportional to square of the amplitude as given in expression (47). However, the increase in amplitude of excitation increases the input strain energy at a higher rate compared to the energy loss due to friction which is linearly proportional to the initial amplitude as given in expression (45), thereby reducing the damping capacity.

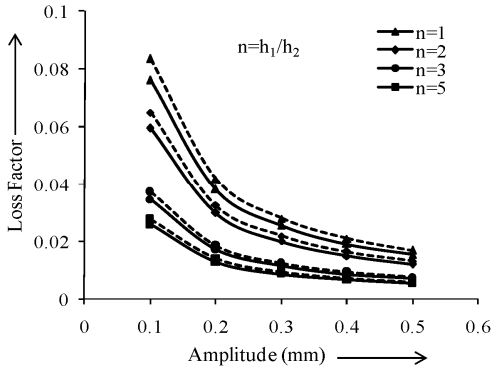

Fig. 19 Variation of loss factor with amplitude for jointed and welded cantilever beams of dimensions=600.6×40.2×6 mm^3

From the Fig. 20, it is concluded that the damping capacity decreases with the increase in thickness. From the expression (47), it is evident that the strain energy introduced in to the system is enhanced with the increase in thickness. Expressions (17) and (42) reveal that the increase in thickness increases the relative slip thereby raising the energy loss. Although the energy loss is enhanced with the increase in thickness, but the damping capacity is reduced as the dissipation of energy is at a slower rate compared to that of the input strain energy.

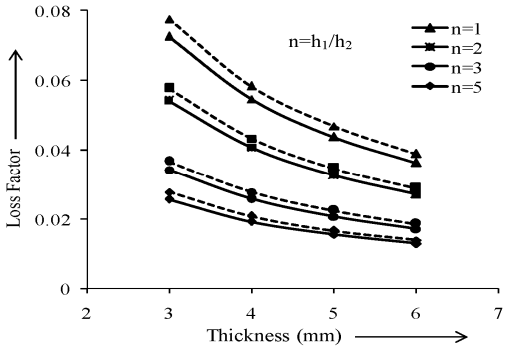

Fig. 20 Variation of loss factor with thickness for jointed and welded cantilever beams of dimensions=600.6×40.2 mm^2 and amplitude=0.1mm

Damping capacity of the layered and welded structures increases with the increase in length as shown in Fig. 21. With the increase in length, the interface area is increased resulting in greater dissipation of the energy due to friction. Furthermore, with increase in length of the jointed beam, strain energy introduced into the system is reduced as evident from the expression (47). Hence, the overall effect is an increase in the damping capacity of the system.

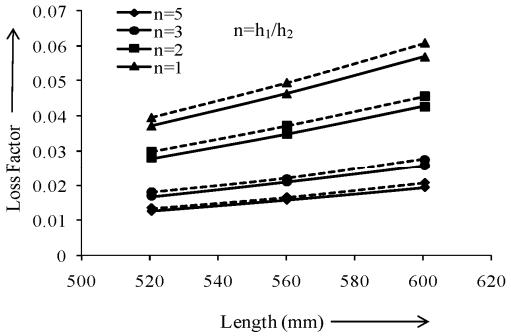

Fig. 21 Variation of loss factor with length for jointed and welded cantilever beams of dimensions=40.2×6 mm^2 and amplitude=0.1mm

VI. Conclusion

A mathematical model for the investigation of the mechanism of slip damping in layered and welded structures with unequal thickness, subjected to dynamic conditions, has been developed. In the present analysis, explicit solutions has been found out for the dynamic response, slip, dissipated energy and loss factor for the welded non-symmetric cantilever beams under both periodic and non-periodic forcing functions of the Heaviside and harmonic type. Proposed mathematical model for damping is validated by conducting experiments. A set of measurements have been taken, which served as a qualitative, experimental validation of the procedure. From the analysis, it is inferred that the damping capacity of layered and welded structures is substantially enhanced by fabricating the structures with symmetric beams. It is also observed that onset of slip is delayed in the structures fabricated with beams of unequal thickness. Energy dissipation is maximized by having the slip interface at the centroid of the total beam cross-section which is the case of jointed beams of equal thickness. Further, it is also deduced that the pressure distribution characteristics, relative slip and kinematic co-efficient of friction at the interfaces, length, thickness, and dynamic amplitude of excitation are the vital parameters influencing the damping capacity of fabricated structures with unequal thickness. The present analysis will help the designers to model the complicated realistic structures in which slip damping is predominant.

References

[1] L. E. Goodman and J. H. Klumpp, "Analysis of slip damping with reference to turbine blade vibration," *Journal of Applied Mechanics*, vol. 23, pp. 421-429, 1956.

[2] L. E. Goodman, "A Review of Progress in Analysis of Interfacial Slip Damping," *Proceedings of the ASME Colloquium on Structural Damping*, New York, pp. 35-48, 1959.

[3] S. W. E. Earles, "Theoretical Estimation of the Frictional Energy Dissipation in a Simple Lap Joint," *Journal of Mechanical Engineering Sciences*, vol. 8, pp. 207, 1966.

[4] A.S. R. Murty, "On damping of thin cantilevers." *Ph.D. Thesis*, Department of Mechanical Engineering, I. I. T., Kharagpur, 1971.

[5] M. Masuko, Y. Ito, and K. Yoshida, "Theoretical analysis for a damping ratio of jointed cantibeam," *Bulletin of Japanese Society of Mechanical Engineers*, vol. 16, pp. 1421-1432, 1973.

[6] N. Nishiwaki, M. Masuko, Y. Ito, and I. Okumura, "A study on damping capacity of a jointed cantilever beam (1st Report; Experimental Results)," *Bulletin of Japanese Society of Mechanical Engineers*, vol. 21, pp. 524-531, 1978.

[7] B. K. Nanda, "Study of the effect of bolt diameter and washer on damping in layered and jointed structures," *Journal of Sound and Vibration*, vol. 290, pp. 1290-1314, 2006.

[8] H. H. Ziada and A. K. Abd, "Load pressure distribution and contact areas in bolted joints," *Institution of Engineers (India)*, vol. 61, pp. 93-100, 1980.

[9] O. Damisa, V. O. S. Olunloyo, C. A. Osheku, and A. A. Oyediran, "Static analysis of slip damping with clamped laminated beams," *European Journal of Scientific Research*, vol. 17, no. 4, pp. 455–476, 2007.

[10] O. Damisa, V. O. S. Olunloyo, C. A. Osheku, and A. A. Oyediran, "Dynamic analysis of slip damping in clamped layered beams with non-uniform pressure distribution at the interface," *Journal of Sound and Vibration*, vol. 309, pp. 349–374, 2008.

[11] B. Singh and B. K. Nanda, "Effect of welding on the slip damping of layered and jointed structures," *Journal of Engineering Mechanics, ASCE*, vol. 136, no. 7, pp. 928–932, 2010.

[12] K. L. Johnson, *Contact mechanics*, Cambridge University Press, New York, 1985.

[13] A.E. Giannakopoulos, T. C. Lindley, S. Suresh, and C. Chenut, "Similarities of stress concentrations in contact at round punches and fatigue at notches: Implications to fretting fatigue crack initiation," *Fatigue Fracture in Engineering Materials and Structures*, vol. 23, no.7, pp. 561–571, 2000.

[14] S. Timoshenko, *Vibration Problems in Engineering*, Van Norstrand Co, Inc, 3rd Edition, pp. 371, 1955.

B. Singh is an Asst. Prof. in the Department of Mechanical Engineering, Sir Padampat Singhania University, Udaipur, Rajasthan, India. He graduated from National Institute of Technology at Kurukshetra, India. He completed his Masters from National Institute of Technology at Rourkela, India. Currently, he is pursuing his research work under the guidance of Prof. Dr. B. K. Nanda. He has teaching experience of more than ten years. He has published 21 papers in international journals and conferences. His research area is structural vibration.

K. K. Agrawal is an Asst. Prof. in the Department of Mechanical Engineering, Sir Padampat Singhania University, Udaipur, Rajasthan, India. He graduated from Government Engineering College, Rewa, India. He completed his Masters from National Institute of Technology, Hamirpur, India. He has teaching experience of more than two years. He has published 2 papers in international and national conferences. His research area is heat transfer and vibration.

B. K. Nanda is a Professor in the Department of Mechanical Engineering, National Institute of Technology at Rourkela, India. He has both teaching and research experience of more than 31 years in the field of machine tool design and structural vibration. He has published more than 75 papers in international and national journals and conferences including Journal of Sound and Vibration, International Journal of Acoustics and Vibration, Journal of Vibration and Control, Structural Engineering and Mechanics: An International Journal, Australian Journal of Mechanical Engineering and Transactions of the Canadian Society of Mechanical Engineering. He has reviewed many papers of international journals like Journal of Sound and Vibration, Transactions of CSME, Trends in Applied Sciences Research and many others. He is a member of the Editorial Board of the journal: Trends in Applied Sciences Research. He has been awarded with many gold medals for his scientific publications.